Hybrid composites · wear · electron microscopy · flammability

E-glass fabric/nano aluminum hydroxide (ATH)/epoxy composites were prepared by manual lay-up and compression molding. An image processing tool was used to quantify fineness of dispersion of nano-ATH particles in epoxy. Fourier transform infrared (FTIR) spectroscopy was used to understand the interaction between nano-ATH and epoxy. Mechanical properties, sliding wear resistance and fire retardance of these composites improved upon addition of nano-ATH. The composite containing 0.125 wt% of nano-ATH exhibited optimum mechanical properties and low specific wear rate.

Einfluss von Nano-Aluminumhydroxid auf tribologische, mechanische und Brennbarkeits-Eigenschaften von E-Glasfaser/Epoxy Multi-Schichtlaminaten

Hybrid-Komposite · Abrieb · Elektronenmikroskopie · Brandverhalten

E-Glasfaser/Nano-Aluminiumhydroxid (ATH)/Epoxy-Komposite wurden durch manuelles einlegen und Formpressen hergestellt. Für die Quantifizierung des Dispersionsgrades von Nano-ATH-Partikeln im Epoxy wurde ein bildgebendes Messverfahren eingesetzt. Die Fourier-Transform-Infrarotspektroskopie (FTIR) wurde benutzt, um die Wechselwirkung zwischen Nano-ATH und Epoxy zu verstehen. Die mit Nano-ATH additivierten Komposite zeigen verbesserte mechanische Eigenschaften wie Abriebwiderstand und Entflammbarkeit. Ein Optimum der mechanischen Eigenschaften und der niedrigen spezifischen Abriebrate weisen die Komposite mit 0,125 Gew.-% auf.

Figures and Tables:
By a kind approval of the author.

Influence of Nano-Aluminum-Hydroxide on tribological, mechanical and Flammability Properties of E-Glass Fabric/ Epoxy Multi-layered Laminates

Polymers reinforced with very small quantities of nano sized particles/fibres/flakes are called polymer nanocomposites. These composites have potential applications in automotive, aerospace and construction sectors due to their excellent structural and functional properties [1]. Nano filler(s) as reinforcement, have many advantages over micro filler(s) in polymer composites. Addition of a small quantity of nano filler(s) in polymer matrix exhibits better properties compared to similar neat polymer or micro filler(s) filled polymer composite [2, 3]. The high specific surface area of nano filler(s) lead to remarkable reinforcing effect and improved adhesion with a polymer matrix even at a small loading. This helps structural integrity and better load transfer capability for nanocomposites [4, 6].

Many researchers used nano fillers (such as TiO_2, ZnO, SiO_2 and carbon nanotubes) as additives to polymer matrices and reported enhanced mechanical and tribological properties [7-9]. Nano alumina and aluminium hydroxide (ATH) were also used as wear resistant fillers in a number of polymer matrices due to their attractive properties like high thermal conductivity, hardness and endothermic decomposition behaviour at elevated temperature. It is reported that addition of nano alumina filler to epoxidized natural rubber (ENR) improves its tensile modulus, hardness and decreases its tensile strength, impact strength and elongation [10]. Qiu et al. [11] reported that Al_2O_3 nanoparticles accelerated curing rate of epoxy and caused an increase in its impact strength and a decrease in wear rate and coefficient of friction. Guang et al. [12] reported that 0.24 vol. % nano-Al_2O_3 filled epoxy composite exhibited lowest specific wear rate and a positive correlation between specific wear rate and impact strength. Also, they found that addition of nano-Al_2O_3 particles to epoxy enhanced the flexural modulus, flexural strength and impact strength of the latter. Shen et al. [13] reported improved ablation resistance with addition of nano Al_2O_3 and $Al(OH)_3$ in epoxy-based composite. But, the performance of $Al(OH)_3$ filler(s) was much better than Al_2O_3. Peng [14] reported that addition of 6 wt.% of $Al(OH)_3$ micro filler to glass reinforced epoxy composite decreased its surface temperature, friction coefficient, and wear loss compared to the neat composite. But, filler content beyond 6 wt% in the composite decreased mechanical property and increased fatigue wear. Dudkin et al. [15] reported that Al_2O_3 nanoparticle/epoxy composites exhibited an increase in mechanical strength and Young's modulus compared to neat epoxy. They recommended a combination of Al_2O_3 nanoparticles and fibres as the optimum reinforcement for epoxy matrix.

Literature reports reveal that structural applications of fabric-reinforced polymer composites increase day by day. Use of nanoparticles could enhance certain functional properties in addition to structural properties of fibre reinforced epoxy based composites. In the present study, glass fabric reinforced epoxy composite

Authors

B. Shivamurthy, Gibin George, K. Udaya Bhat, S. Anandhan, Karnataka, India

Corresponding Author:
S. Anandhan
Department of Metallurgical and Materials Engineering,
National Institute of Technology Karnataka,
Srinivas Nagar, Mangalore-575025, Karnataka, India
Phone: +91-824-2474000
Fax: +91-824-2474059
E-Mail: anandtmg@gmail.com

KGK RUBBERPOINT

Discover more interesting articles and news on the subject!

www.kgk-rubberpoint.de

Entdecken Sie weitere interessante Artikel und News zum Thema!

1 Technological properties of the matrix and reinforcement used for fabrication of the composites

Epoxy resin (LAPOX L-12)		Hardener (LAPOX K-13)		E-Glass fabric	
Colour	0.8 GS	Color	0.8 GS	Areal density(g.m-2)	201-203
Epoxy value	5.35 Eq./kg	Viscosity @ 25°C	10 M Pa	Thickness (mm)	0.17-0.19
Viscosity @ 250C	11850 M Pa	Pot Life @ 80°C	69 min	Ash content (%)	33
Volatile content @1050C, /Hr.	0.4 %	Gel time @ 80°C	118 min	Moisture (%)	0.22
Hydrolysable chlorine	0.08 wt.%			Thread count: Warp (No.)	160
Martens Value	150 °C			Weft (No.)	130

and glass fabric reinforced nano-ATH filled epoxy composites were prepared; their mechanical properties, sliding wear behaviour and flammability behaviour were investigated. Also, the wear rates and mechanical properties of these composites were correlated. Fourier transform infrared (FTIR) spectroscopy was used to understand the interaction between nano-ATH and epoxy and the influence of nano-ATH on the cure behavior of epoxy. Filler dispersion in these hybrid composites was quantified by using an image analysis tool and it was used along with the FTIR spectroscopy results to understand the trends in mechanical properties and wear behaviour of these composites.

Experimental

Materials

Composite laminates were fabricated using a bi-directional, plain-woven E-glass fabric (with an areal density of 200 g.m^{-2}) obtained from Montex glass fibre India Pvt. Ltd., India, as the reinforcement. Bisphenol-A based epoxy resin (LAPOX L-12), hardener (LAPOX K-13) and accelerator (DY06) were purchased from M/s Atul Ltd. Valsad, Gujarat, India. Nano-ATH was obtained from US Research Nanomaterial Inc. USA, (product ID: US3026, Purity: 99.9 % and average particle size: 10-20 nanometres). The technological properties of resin, hardener and glass fabric used for fabrication of composite laminates are mentioned in Table 1.

Fabrication of composites

The matrix was prepared by mixing a v/v ratio 5:4 of epoxy resin and hardener at 60 °C by a magnetic stirrer. Accurately weighed nano-ATH was added manually to the matrix maintained at 100 °C. It was continuously stirred for 4 h at an rpm of 1200, using a magnetic stirrer. The mixture of nano filler, hardener and epoxy resin was passed in an indigenous three roll calendaring mill. The gap between the 50 mm diameter ceramic rollers in the mill was kept around 5 µm and the rotational speeds of the first, second and third rollers were kept at 50, 100 and 200 rpm, respectively. The mix collected at the outlet of the three roll mill was fed in to the inlet of the mill 5 times to obtain a homogeneous mix and uniform dispersion of nano-ATH particles in the matrix. To the matrix 2 wt. % of accelerator was added followed by constant stirring for 5 minutes using a magnetic stirrer. Three batches of matrices consisting of 0.125, 0.25 and 0.5 wt. % of nano-ATH were prepared separately by the above method. Figure 1 shows the schematic of three roll mill used for preparation of nano-ATH/epoxy masterbatch.

The masterbatch was coated on to each layer of E-glass fabric by a brush and a roller. Sixteen such layers were kept between the pressing platens of hydraulic press at a stacking sequence of [(0/90)]8. Thick polyester films were used for mould release and to obtain smooth composite slabs. Resin impregnated fabric stock was pressed in hydraulic press (capacity 40 T) at a pressure of 0.5 MPa for 2 h at 140 °C. The prepared composite slabs having a size of 250 mm × 250 mm × 3 mm were post cured for 8 h at 140 °C and their compositions are shown in Table 2.

2 Compositions of neat and nano-ATH filled glass/epoxy composites

Sample ID	Quantity of constituents (wt. %)		
	Nano ATH	Resin	E-glass fabric
GEC	0	50	50
0.125ATHGEC	0.125	49.875	50
0.25ATHGEC	0.25	49.75	50
0.5ATHGEC	0.5	49.5	50

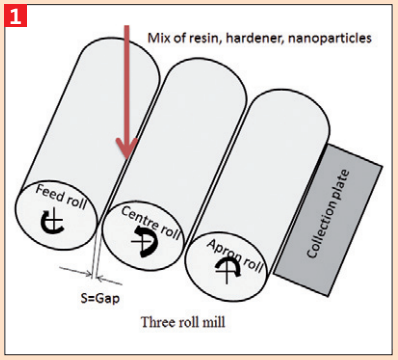

Fig. 1: Schematic of three roll mill.

Experimental methods

The FTIR spectra of the neat ATH, glass fabric, epoxy, glass/epoxy and glass/epoxy/nano-ATH composites were recorded in attenuated total internal reflectance (ATR) mode by using a FTIR spectrometer (Jasco 4200 FTIR spectrometer, Japan). The scans were made in a wave number range of 4,000 - 650 cm^{-1} and the averages of 32 scans were recorded for each sample. The neat and nano-ATH filled glass fabric/epoxy composites were characterized as per ASTM standards to estimate the physical and mechanical properties. Actual densities of the composites were measured according to ASTM: D792 (displacement method) [16]. Vickers hardness of the composite specimens was measured by using a Matsuzawa microhardness tester (Model No MMT-X7A, Japan). Tensile behaviour was investigated as per ASTM: D638 by Universal Testing Machine (Instron 3366, UK) [17]. A three point bending technique was adopted to investigate flexural properties of the composites as per ASTM: D790 [18]. The interlaminar shear strength (ILSS) was investigated according to ASTM: D2344 (short beam shear test method) [19]. In each case, to evaluate the physical and mechanical properties, five samples were tested and the average values are reported.

As per ASTM: G99, pin-on-disc wear test apparatus was used to investigate sliding wear behavior of the composite laminates [20]. The sliding speed and

sliding distance were fixed as 3.5 $m.s^{-1}$ and 1.5 km, respectively. The normal load was varied as 15, 30 and 45 N. In each case, the final weight of the specimen was accurately measured and the wear loss (w) was estimated as the difference of initial weight (w_1) and final weight (w_2). The specific wear rate K_s ($g.N^{-1}.m^{-1}$) was calculated by Eq.1.

$$K = \frac{W}{F_n \times d} \quad (1)$$

Where W is the wear loss (g); F_n is the normal load (N), and d is the sliding distance (m). The coefficient of friction (μ) was calculated by Eq.2.

$$\mu = \frac{F_f}{F_n} \quad (2)$$

Where, F_f is the frictional force (N).

A scanning electron microscope (SEM) (JSM-6380LA, JEOL, Japan) was used to evaluate the texture and morphology of the glass fabric, cross sectional views across the thickness of the laminates. In order to assess the fineness of dispersion of nano-ATH in the epoxy matrix, aluminum elemental mapping of the broken surfaces of the hybrids was carried out using energy dispersive X-ray (EDX) (Link ISIS-300 Microanalytical System, Oxford instruments, UK) facility of the SEM. The samples were cut in to 5 mm × 5 mm squares and sputtered with gold in a sputtering unit (JEOL JFC 1600), auto fine coater, to make them conductive. The elemental composition maps (EDX map) of the sample surfaces were then taken at a suitable accelerating voltage, for the best possible resolution using the SEM. The elemental dot maps were analyzed by Image–J Software [21, 22]. The morphologies of worn out surfaces of the wear test samples were investigated by SEM to understand wear mechanism.

The limiting oxygen index (LOI) test (ASTM: D2863) is a widely used research and quality control tool for determining the relative flammability of polymeric materials [23]. The LOI of the neat and nano-ATH filled composites were determined by using a LOI analyzer (Dynisco, USA). A numerical index, the 'LOI', is defined as the minimum concentration of oxygen in an oxygen–nitrogen mixture, required to just support downward burning of a vertically mounted test specimen. Hence, higher LOI values represent better flame retardance. LOI was calculated by using the following formula:

$$LOI(\%) = \frac{[O_2]}{[O_2] + [N_2]} \times 100 \quad (3)$$

Where, $[O_2]$ is the volumetric flow rate of oxygen (cm^3/sec) and $[N_2]$ that of nitrogen. Five samples of 6.5 mm × 3.2 mm ×150 mm were tested and the average values were taken to estimate time-to-ignition, flame propagation rate and LOI required for burning the composite specimens.

The UL-94 vertical flammability test was performed according to ASTM: D3801 [24] with the specimen dimensions of 12.5 mm×5 mm ×150 mm. In this case, 10 samples were tested, duration of burning after every ignition trial of individual samples was noted and mean time of burning after ignition was estimated.

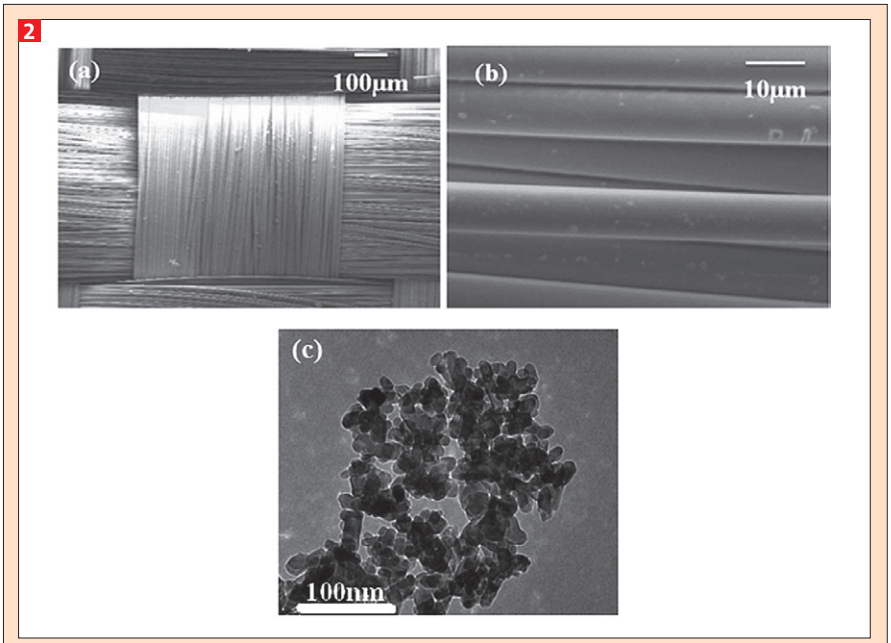

Fig. 2 SEM micrographs of a) plain-woven E-glass fabric, b) individual glass fibers, and c) TEM micrograph of nano-ATH.

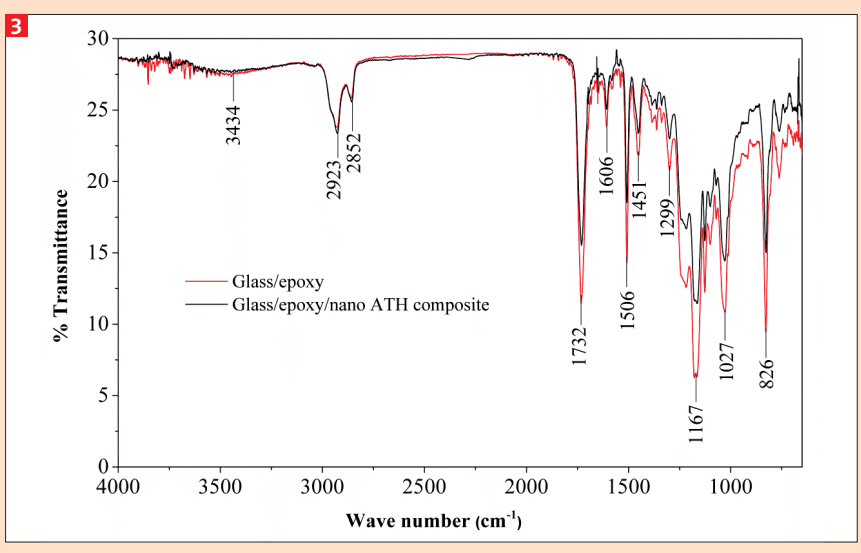

Fig. 3 FTIR spectra of glass/epoxy and glass/epoxy/nano ATH composites.

Results and discussion

Morphology of the glass fabric and nano-ATH

The scanning electron micrographs of plain-woven E-glass fabric and fibers used in the fabric are shown in Figure 2 (a) and (b), respectively. It is confirmed that the fabric is of the bi-directional plain woven type and fibres are clean and defect free. Figure 2(c) shows the

TEM micrograph of the nano-ATH (courtesy: US Research nanomaterials Inc., USA), in which agglomerated nanoparticles of ATH can be seen. These nanoparticles have an elongated structure with low angularity and an average size of 10-20 nm.

FTIR spectroscopy

A comparison of the FTIR spectra of glass/epoxy composite and glass/epoxy/nano-ATH composite is shown in Figure 3. The peaks at 3452 cm^{-1} are due to O–H stretching and the peaks at 2965 and at 2873 cm^{-1} are attributed to the symmetric and asymmetric vibrations C–H in CH_3, respectively. The peak at 1732 cm^{-1} is assigned to C=O stretching and the peak at 1606 cm^{-1} corresponds to C=C stretching in aromatic rings. The peak at 1506 cm^{-1} is due to the C–C stretching in aromatic rings and the one at 1451 cm^{-1} is attributed to aromatic C=C–C stretching. The peaks at 1299, 1167, 1027 and 826 cm^{-1} correspond to C–O stretching in oxirane ring, anti-symmetric vibrations of C–H, Stretching C–O–C of ethers and C–O–C stretch of oxirane group, respectively [25].

The peak positions of the glass/epoxy composite and glass/epoxy/nano-ATH composite remain the same, but, there is a distinct change in the intensity of the peaks at the finger print region due to the change in the degree of curing [26]. The reduction in intensities, particularly for the peaks corresponding to the oxirane ring in glass/epoxy/nano-ATH composite is due to the reduction in the number of oxirane rings in the composite. Therefore, it is assumed that more oxirane rings are consumed during the curing process, when nano-ATH is added to glass/epoxy composite. The consumption of oxirane rings is a measure of the degree of curing [27]. Thus, it can be said that there is an improvement in the cross-linking in the epoxy by the addition of nano-ATH. It is presumed that, in the early stages of cure, the hydroxyl groups in nano-ATH can act as the initiator for the reaction [28]. The approximation on the utilization of the hydroxyl group on nano-ATH is confirmed from the FTIR spectra (Figure 4), where the FTIR spectra of nano-ATH, glass/epoxy composite, glass/epoxy/nano-ATH composite, glass fabric and epoxy are stacked together. It can be observed that the broad O–H stretching peak at 3453 cm^{-1} corresponding to the nano-ATH particles is absent in glass/epoxy/nano-ATH composite,

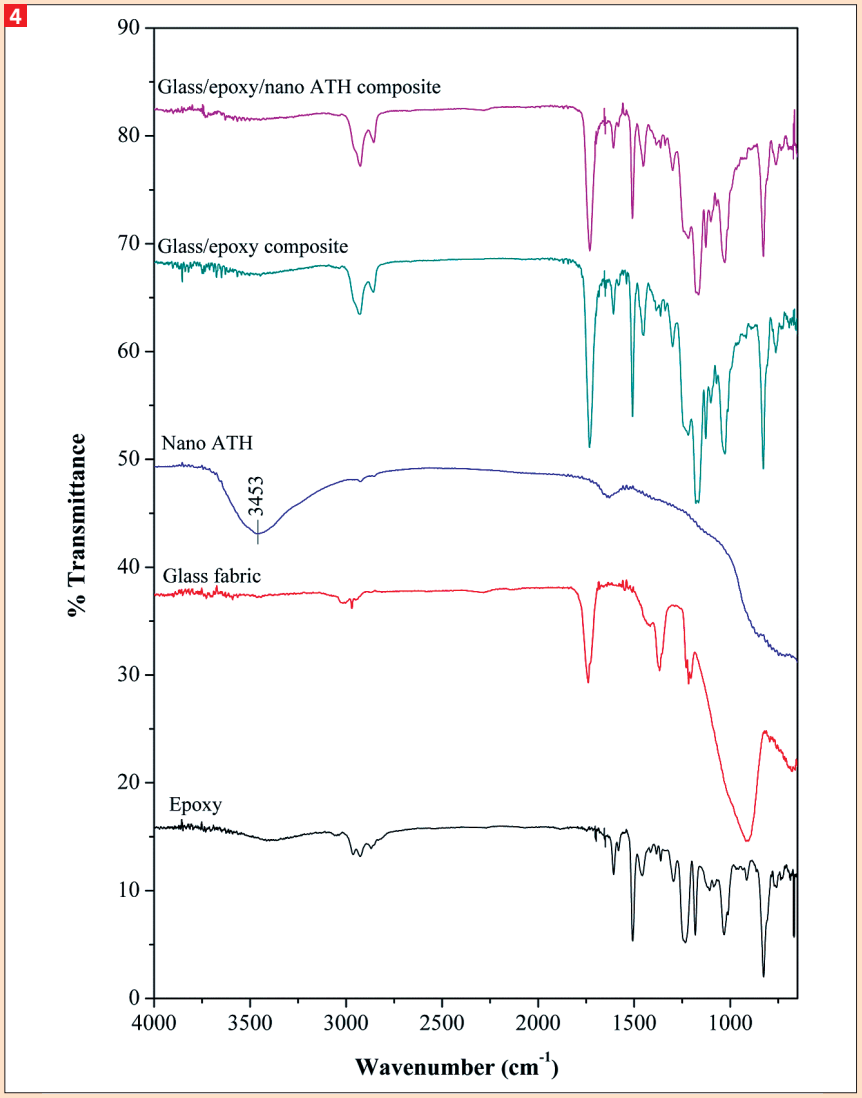

Fig. 4 FTIR spectra of epoxy, glass fabric, nano-ATH, glass/epoxy composite and glass/epoxy/nano ATH composite.

thus supporting the assumption made earlier. From the ongoing discussion it can be understood that the interaction between nano-ATH and epoxy not only helps the crosslinking process of the latter, but, also leads to a good interface development between ATH and epoxy.

Analysis of degree of dispersion of nano-ATH particles in the composite samples

The elemental composition maps of the composites are shown in Figure 5. Each EDX map was divided into 400 µm × 400 µm sample area and analyzed by Image-J software to estimate the fineness of dispersion of nano-ATH particles. The number density distribution measurements technique (or sparse sampling or grid quadrant counting) was adopted to analyse the degree of dispersion of the nano-ATH particles in the epoxy matrix [22]. The results have been plotted as number of particles versus area for nano-ATH filled composites (Figure 6). In this technique, the number of particles in the neighbouring grids with unit area is counted and the degree of inhomogeneity of dispersion is quantified as the standard deviation (σ). The standard deviation among the number of particles per unit area was estimated by the following equation:

$$\sigma = \sqrt{\frac{1}{n}\sum_{i}\left(N_{Ai} - \overline{N_A}\right)^2} \qquad (4)$$

Where, N_{Ai} is the observed number of inclusions per unit area in the i^{th} location, $\overline{N}_A$ is the average number of particles in unit area. The maximum homogeneity is characterized by the minimum standard deviation and the degree of homogenei-

ty is increased with decrease in the standard deviation.

From the aluminium EDX maps of the composites (Figure 5) it is observed that the dispersion of ATH nanoparticles is uniform in 0.125 and 0.25 wt. % nano-ATH filled composites. In the 0.5 wt. % nano-ATH filled sample, agglomeration of nano-ATH particles is observed. Also, the quantitative results obtained by image processing (Figure 6) for 0.125 and 0.25 wt. % ATH filled composite samples exhibit standard deviations of 6 and 8, respectively. In contrast, the 0.5 wt. % ATH filled composite sample shows a standard deviation of 36, indicating the clustering of ATH particles. From the ongoing discussion, it can be understood that by three roll mill mixing process relatively uniform distribution of ATH nanoparticles can be achieved only at a lower filler content and 0.25 wt. % of nano-ATH is the optimum filler loading for these hybrid composites.

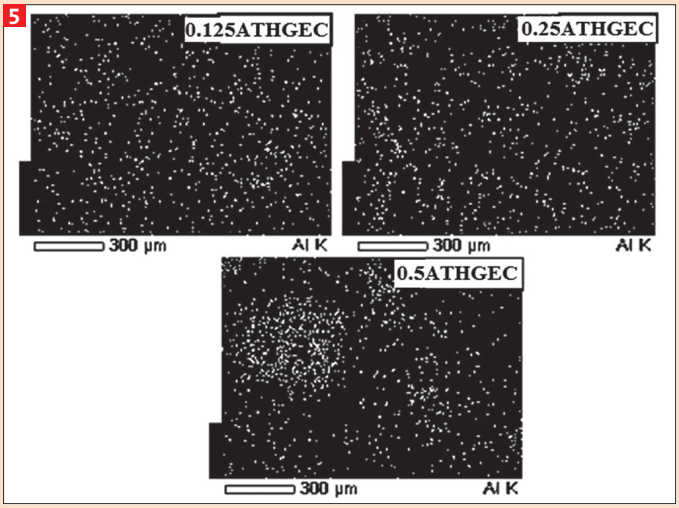

Fig. 5: Elemental dot maps of aluminium of the nano-ATH/glass/epoxy laminate surfaces.

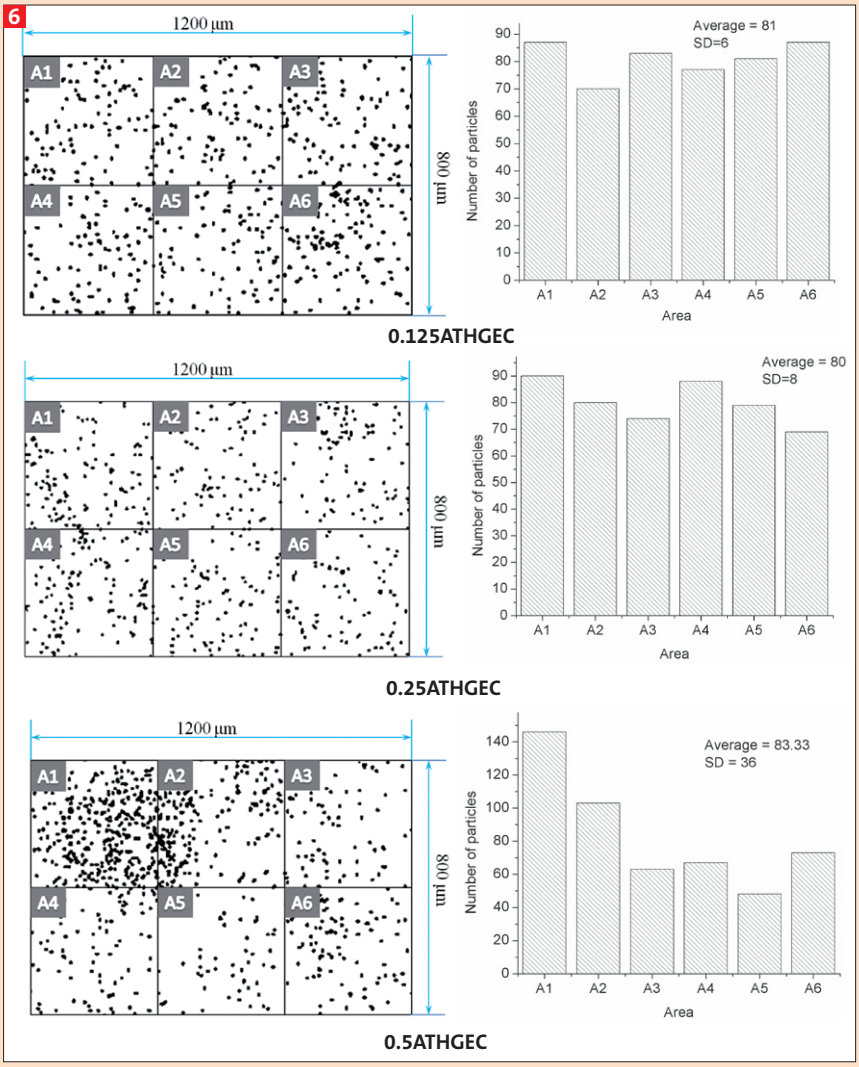

Fig. 6: Nano-ATH particle distribution and dispersion in nano-ATH/glass/epoxy composites.

Further, the samples that were used for the estimation of degree of dispersion of nano-ATH were cut by a diamond tipped cutter, the morphology of the cross sections were analysed by a scanning electron microscope. The SEM micrographs of the cut sections of the laminates are shown in Figure 7. Good adhesion between the epoxy matrix and reinforcement was observed in the neat and the hybrid composite laminates containing 0.125 wt. % and 0.25 wt. % of ATH. Poor interface along with cavities were observed in 0.5 wt. % ATH filled composite laminate. These cavities have formed in the laminate due to dislodgement of loosely packed, agglomerated and poorly impregnated nano-ATH from the surface during cutting.

Mechanical properties

Vickers hardness

Mechanical properties of glass fabric/epoxy composites both with and without nano-ATH are shown in Table 3. It is clear that the hardness of the glass epoxy composite laminates improved by the addition of nano-ATH up to 0.25 wt. %. This is because of the good dispersion of nano-ATH particles in the epoxy matrix at a lower loading. The small particle size combined with the low angularity of the nano-ATH particles favours uniform distribution of them between individual fibres and in between the fabric layers, promoting more resistance to matrix deformation. Also, the nano-ATH particles being harder than the epoxy matrix, take up the compressive stress on the matrix, enhancing the lateral non-deformability of the composite when a load is applied. But in 0.5ATHGEC, due to agglomeration of particles, improper wetting and poor interface, the hardness is lower and inconsistent.

However, all the nano-ATH filled glass fabric reinforced epoxy composites are harder than the neat composite implying the importance of adding nano filler(s) to the matrix.

Tensile properties

The tensile strength (σ_t), Young's modulus (E_t) and percentage of elongation at break (e) of the composites are shown in Table 3. Tensile behaviours of all the composites are represented as load versus elongation curves (Figure 8). It is observed that due to addition of nano-ATH filler (0.125 and 0.25 wt. %) to epoxy matrix, the values of tensile strength and ultimate elongation of the glass/epoxy composites are improved and the Young's modulus changes marginally. Similar results were reported by Dudkin et al for nano Al_2O_3 particulate filled epoxy [15]. Addition of rigid nano-ATH filler to glass/epoxy composites, changes their nature from brittle to strong and tough. The nano filler particles in the interface region between the fibre and matrix makes the latter tougher and hinders propagation of cracks in the matrix. The reinforcing effect of the nano-ATH particles in the interface zone helps in effective load transfer between the matrix and the reinforcement.

The hybrid composite, 0.5ATHGEC, exhibits a lower tensile strength but similar range of elongation comparable to that of the other systems. This is attributed to deterioration in the load bearing capability due to stress concentration at filler agglomerated zones. Hence, from structural point of view, the 0.125 to 0.25 wt. % nano-ATH loaded composites exhibit better tensile properties.

7

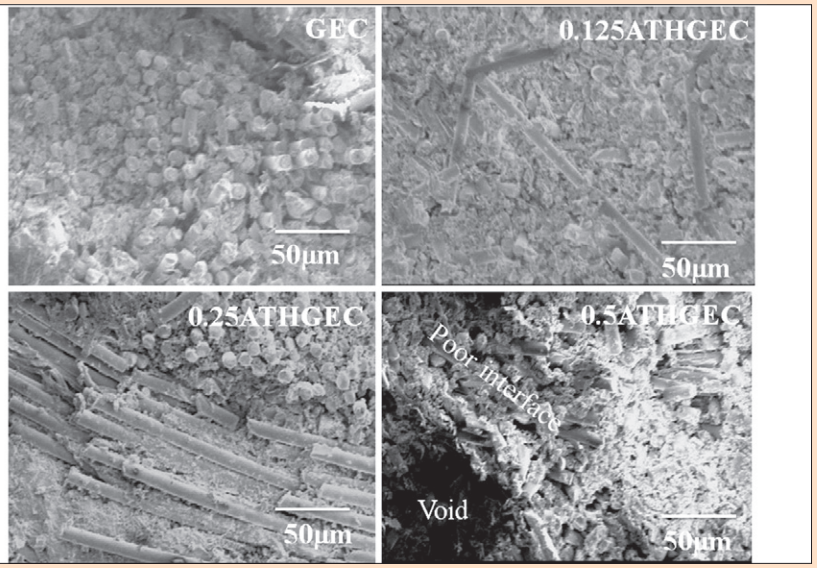

Fig. 7: SEM micrographs of the cross sections of the neat and nano-ATH filled glass/epoxy composite slabs.

3 Mechanical properties of neat and nano-ATH filled glass/epoxy composites.

Sample ID	σ_t (MPa)	E_t (GPa)	e (%)	σ_f (MPa)	E_f (GPa)	τ (MPa)	HV (MPa)	$(\sigma\ e)^{-1}$
GEC	312 ±3	8.1±0.3	5.6	332±3	20.6±0.3	13.6±0.2	25.6±2	7.63E-04
0.125ATHGEC	398 ±3	8.4±0.3	6.8	403±3	22.1±0.3	18.2±0.2	60.5±2	3.69E-04
0.25ATHGEC	405 ±3	8.4±0.3	6.2	391±3	24.3±0.3	17.8±0.2	63.3±2	3.98E-04
0.5ATHGEC	407 ±3	8.6±0.3	6.2	288±3	22.4±0.3	16.0±0.2	38.4±2	3.96E-04

During tensile testing, delamination was observed before fracture in 0.5ATHGEC, whereas in other samples a purely tensile failure was observed. This could be attributed to poor interface formation in 0.5ATHGEC.

Flexural properties and Inter laminar shear strength

The flexural and inter laminar shear properties are shown in Table 3. The flexural strengths and flexural moduli are improved by the addition of nano-ATH in the hybrid composites. This is because the filler nanoparticles restrict the movement of fabric layers when the specimen is subjected to a bending load. But, at a higher filler content, the effectiveness of this reinforcement is reduced by agglomerated particles, improper wetting and poor interface. Also, increased toughness by the addition of nano-ATH to epoxy

8

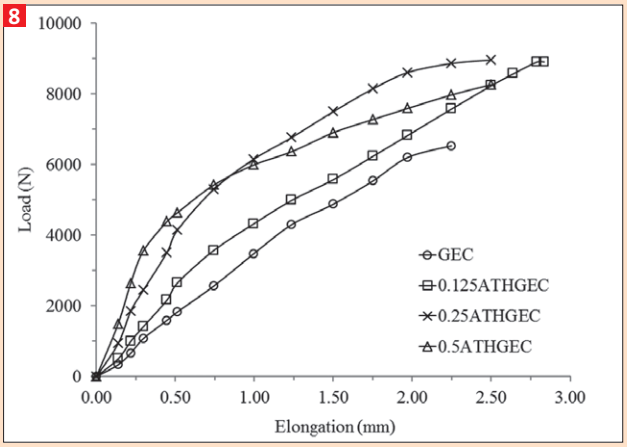

Fig. 8: Tensile load versus elongation curves of the neat and nano-ATH filled glass/epoxy composites.

9

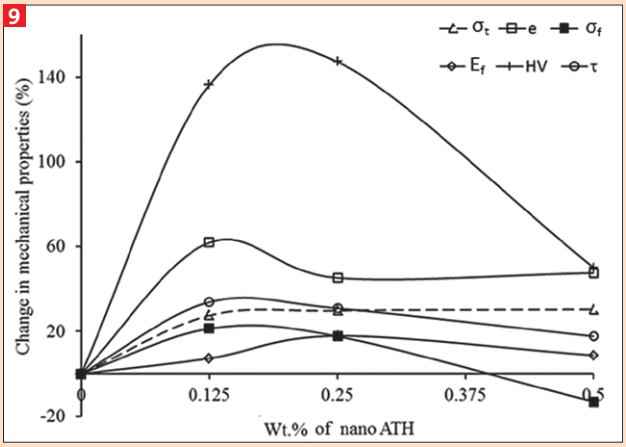

Fig. 9: Effect of nano-ATH content on the mechanical properties of glass/epoxy composite laminates.

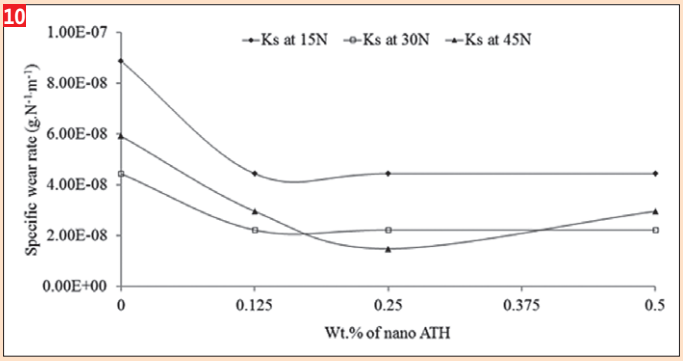

Fig. 10 Specific wear rates of the neat and nano-ATH filled glass/epoxy composites at normal applied loads 15, 30 and 45 N.

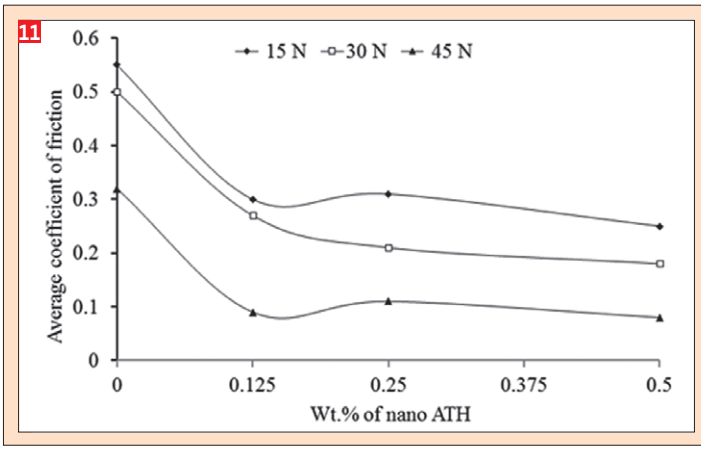

Fig. 11 Average coefficients of friction of the neat and nano-ATH filled glass/epoxy composites at normal applied loads 15, 30 and 45 N.

matrix contributes to the enhancement of ILSS of the composites.

The influence of nano-ATH filler on mechanical properties is plotted as percentage change in mechanical properties versus content of filler in the hybrid composites (Figure 9). All the mechanical properties considerably improve by the addition of 0.125 and 0.25 wt. % of the nano filler. But, at a higher filler loading, only a marginal improvement in the matrix-dominant properties like hardness and ILSS was observed.

Specific wear rate and coefficient of friction

The specific wear rates and average coefficient of friction of the neat and nano-ATH filled glass fabric epoxy composites, for a fixed sliding distance of 1.5 km under loads of 15, 30 and 45 N at a constant sliding velocity of 3.5 $m.s^{-1}$ are shown in Figure 10 and 11, respectively. The nano-ATH filled glass fabric/epoxy composites exhibit the lowest wear rates under all the loads compared to the neat glass fabric/epoxy composite. About 50 % reduction in wear rate is obtained by the addition of nano-ATH to the epoxy/glass composite. The 0.125 and 0.25 wt. % nano-ATH filler loaded composites exhibit lower wear rates as compared to the neat and 0.5 wt. % nano-ATH loaded composites. This is due to the optimum mechanical properties and good structural integrity of those composites having lower filler content. From this observation, it can be concluded that the specific wear rates of the present composite systems strongly depend on the mechanical properties. Addition of an appropriate amount of nano-ATH powder to epoxy/glass composites could increase their resistance to wear and friction.

In nano-ATH loaded glass/epoxy composites subjected to sliding action, the wear rate is less compared to that of the neat one due to the following reasons: the nano-ATH particles in the composites absorb heat and decrease the surface temperature, friction coefficient, and wear rate of the composites. The nano-ATH particles dislodged from the sliding surface get blended with the wear debris and thereby strengthen the film that forms on the sliding surface. The lower angularity of the nano-ATH particles provides lower abrasiveness in sliding action and leads to pure adhesive wear. Also, nano-ATH particulates in the composites are smaller as compared to the particles worn out from the epoxy matrix. Hence, the rate of material removal due to sliding wear in nano particulate filled composites would be much less. The hybrid composite that contains the optimum loading of nano-ATH exhibits the best mechanical properties along with the lowest wear rate and coefficient of friction.

Correlation of mechanical properties with wear

In literature, it is reported that specific wear rates of polymer composites depend on their mechanical properties. Peng et al reported that the optimum content of micro-ATH particles in epoxy imparts the best wear resistance and lowest coefficient of friction along with better mechanical properties compared with that of neat epoxy [14]. Ji et al reported that wear resistance of nano-alumina/epoxy composites depended on the strength of the interface between the filler and the matrix [11]. Dudkin et al reported that nano-alumina filler and nano-alumina fibre increased the strength and modulus, respectively, of an epoxy matrix. Both these effects increased the wear resistance of epoxy [15]. Shi et al have shown a positive correlation between wear resistance and impact strength of epoxy filled with nano-sized Al_2O_3 particles [12]. Also, a few researchers have correlated the Ratner-Lancaster factor [29, 32] with wear resistance of polymer matrix composites. Lancaster factor is an inverse of the product of tensile strength (σ) and percentage elongation (e) of a polymer composite. The results of Bijwe et al. [29] on polyethersulfone/aramid composites revealed that the specific wear rate had a linear relationship with the Ratner-Lancaster factor. From literature, it was observed that as the tensile strength and elongation increase, the fracture toughness of a material increases, and more energy is required to deform the material; hence, its wear rate decreases [30, 31 and 32]. A similar observation has been made in the present study too. Figure 12 shows the $(\sigma.e)^{-1}$ factor and specific wear rate versus content of nano-ATH of the glass/epoxy composites under study. From Figure 12, it is observed that the nano-ATH filled glass/epoxy composites exhibits the lowest value of $(\sigma.e)^{-1}$ and the lowest specific ware rates (at all the three applied loads) compared to the neat glass/epoxy composite. The tensile strength and elongation increase upon addition of an optimum quantity of the nano-ATH filler to the glass/epoxy com-

posites. It also increases the fracture toughness, in addition to the other mechanical properties. Hence, wear rates of 0.125 and 0.25 wt. % nano-ATH loaded composites decrease. As the filler loading is 0.5 wt. %, it deteriorates the hardness, ILSS and flexural properties, but, the toughness remains more or less a constant. Hence, due to synergism of properties it gives slightly lower wear resistance compared to 0.125 ATHGEC and 0.25 ATHGEC. Also, nano-ATH filler loaded composites have lower values of Lancaster factor than neat glass/epoxy composites, hence, considerable reduction in wear rate was observed in the hybrid composites at all levels of filler loading.

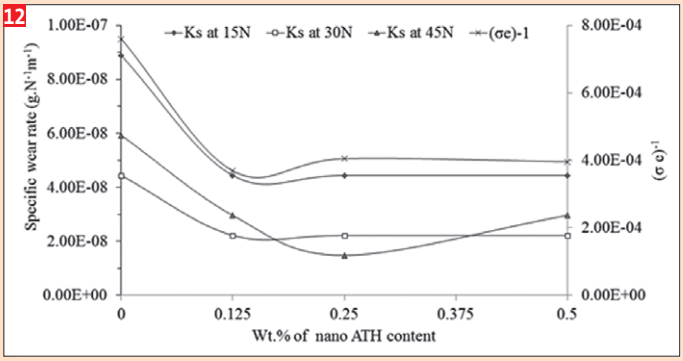

Fig. 12 (σ. e)-1 factor and specific wear rate versus nano-ATH content of the hybrids.

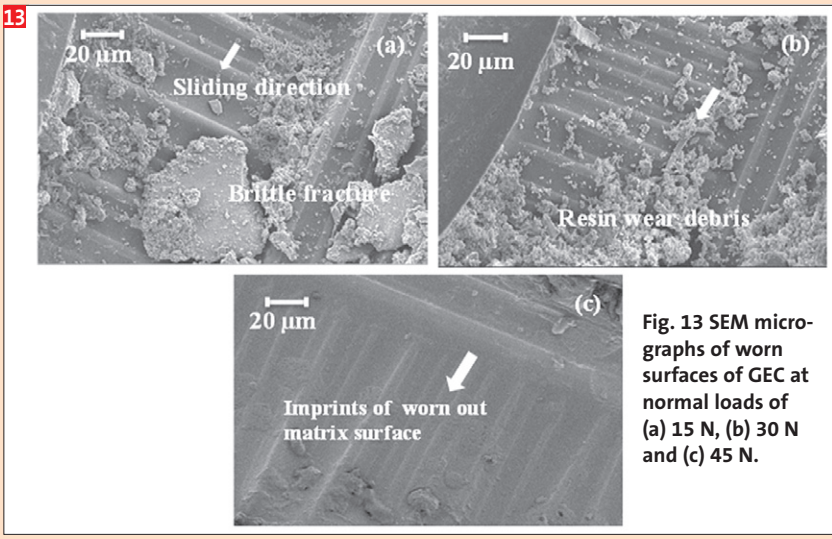

Fig. 13 SEM micrographs of worn surfaces of GEC at normal loads of (a) 15 N, (b) 30 N and (c) 45 N.

Mechanism of wear

Worn out composite sample surfaces were imaged by SEM microscopy to understand the mechanism of wear of the neat glass/epoxy composite and its nano-ATH loaded counterparts. It is found from the SEM micrographs that the top matrix layer of the neat glass/epoxy composite is heavily damaged due to brittleness of the top epoxy layer. This brittle fracture of the epoxy layer develops debris of varying sizes (Figure 13 (a)), which get trapped between the sliding surfaces, creating further abrasive wear in addition to adhesive wear. Further, the large debris get crushed and displaced from the wear surface at higher loads (Figures 13(b) and 13(c)).

SEM micrographs of the worn out surfaces of 0.125ATHGEC are shown in Figure 14. In this case, mild wear is observed due to plastic deformation of top layer of the nano-ATH filled hybrid composite. The wear debris was smaller and uniform in size as compared to the neat glass/epoxy composite. The smaller wear debris undergoes plastic deformation and adheres to the counter surface. This develops a film between the abrading and composite surfaces, which in turn, reduces the wear. Also, ploughing could be observed at higher loads (Figure 14(c)). However, the depth of these plough lines is lower, due to small and uniform wear debris. Similar type of plastic deformation and worn out surface morphology are observed in 0.25ATHGEC surfaces (Figure 15). Morphology of worn out surfaces of 0.5ATHGEC are shown in Figure 16. The worn out surfaces show that the material removal from the surface is in the form of mild delamination (Figure 16 (c)). Further, a thin delaminated layer between the contact surfaces is responsible for the uniform contact between the latter. It distributes the load uniformly throughout the contact surface and reduces the wear at higher loads. Poor interface between the fiber and matrix is observed at a higher content of nano-ATH.

Flammability properties

Even though glass fiber-reinforced epoxy composites have excellent mechanical properties and corrosion resistance, they have some limitations in applications that demand fire retardance. This affects the structural integrity of the glass fiber-reinforced epoxy-based composites

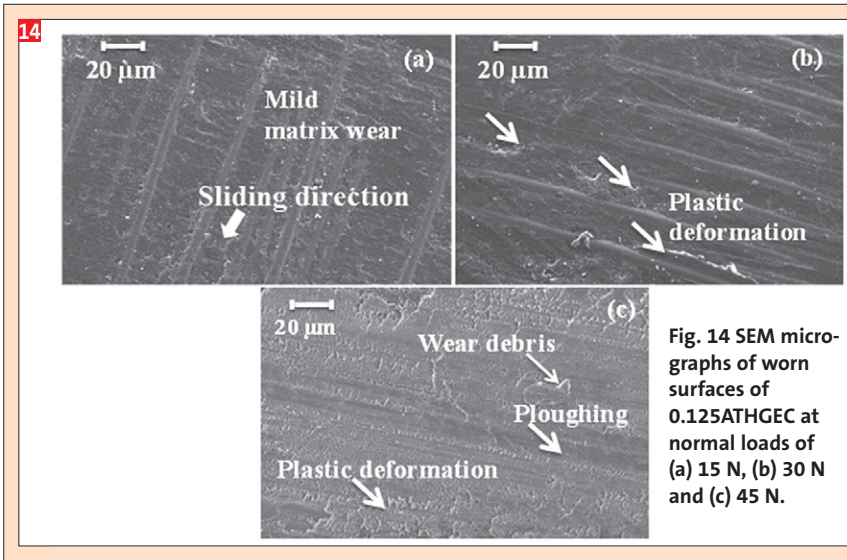

Fig. 14 SEM micrographs of worn surfaces of 0.125ATHGEC at normal loads of (a) 15 N, (b) 30 N and (c) 45 N.

15

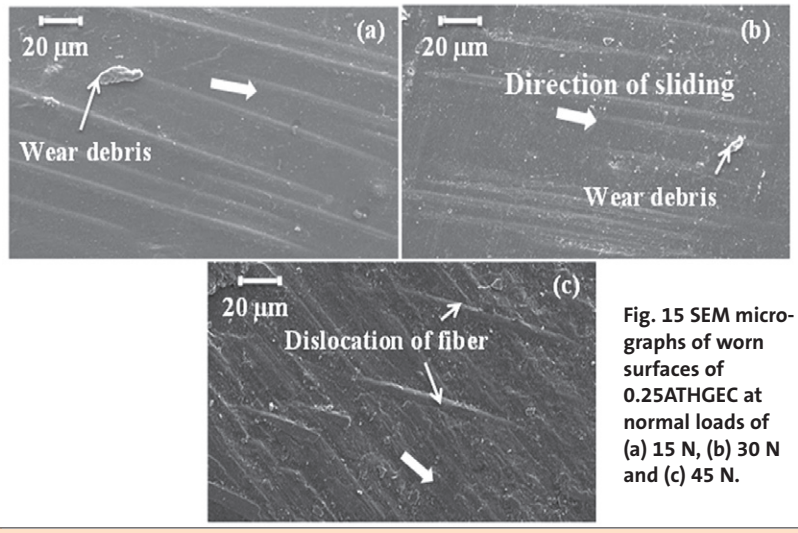

Fig. 15 SEM micrographs of worn surfaces of 0.25ATHGEC at normal loads of (a) 15 N, (b) 30 N and (c) 45 N.

when exposed to fire. Hence, to enhance the flame-retardance of glass/epoxy composites, many researchers have used flame retardants to modify the flammability of epoxy resin and found improved fire-retardance for the resulting compositions [33, 34]. Hydrated minerals, such as ATH are potential fire-retardant fillers suitable for both thermoset and thermoplastics. The effect of nano-ATH filler on the fire-retardance of the glass/epoxy composites was investigated by LOI and UL-94 vertical flammability method and the results are shown in Tables 4 and 5. The LOI values increase marginally with an increase in the nano-ATH content. Also, the UL94 rating values show a similar trend.

Due to the addition of nano-ATH particles, fire-retardance of glass/epoxy composites has been improved. This can be attributed to the endothermic decomposition of nano-ATH filler at temperatures exceeding 200 °C. Decomposition of ATH releases water molecules, which cools down the polymer surface and delay further ignition of the polymer. Also, this process dilutes the combustible gases when the composites are subjected to fire and thereby reduces the flammability [35]. The 0.5 wt. % filler loaded glass/epoxy composites exhibit better fire retardance compared with the other composites because of its higher nano-ATH content.

According to UL rating, the fire retardance of a polymer is classified as V-0 (specimens not burning for more than 10 seconds and the drip do not ignite the cotton), V-1 (specimens not burning for more than 30 seconds and the drip do not ignite the cotton), V-2 (specimens not burning for more than 30 seconds and the drip ignite the cotton). If the entire sample is consumed, then it is classified as non-rated (NR). The UL-94V rating of the neat and nano-ATH filled glass/epoxy composites are shown in Table 5. The UL-94 rating changes from NR to V-0 even at a loading of 0.25 wt. % of nano-ATH. This is a remarkable improvement in the flame-retardance of the epoxy/glass composites.

This study proves that nano-ATH improves not only the mechanical properties and wear behavior, but, also the fire retardance of the glass/epoxy composites.

16

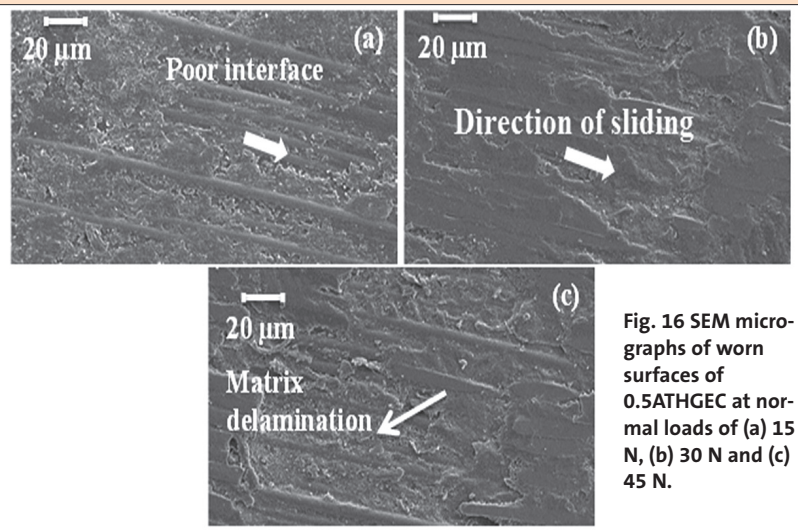

Fig. 16 SEM micrographs of worn surfaces of 0.5ATHGEC at normal loads of (a) 15 N, (b) 30 N and (c) 45 N.

Conclusions

Addition of nano-ATH to multi-layered laminates made of glass fabric/epoxy composites makes the material tougher and more rigid. Also, the flexural strength, interlaminar shear strength and hardness of the hybrid composites improved due to better interface and uniform dispersion of nano-ATH particles at a lower filler content. The hybrid composites that contain 0.125 and 0.25 wt. % of nano-ATH, exhibit better tensile strength and toughness in addition to other mechanical properties. Also, the wear rate and coefficient of friction is lower in these two composites. A further increase in the nano-ATH content slightly deteriorates the mechanical properties and specific wear rate. Based on the experimental results it is found that, the specific wear rate depends on toughness of the material. The lowest Ratner-Lancaster factor of these composites signifies the lowest specific wear rate. This study also proves that nano-ATH improves not only the mechanical properties and wear behavior, but, also the fire retardance of the glass/epoxy composites.

References

[1] C. Oncel, F. Smith (2001) The physics and chemistry of solids in nanostructures, John Wiley, New York.
[2] M. G. Kim, J. S. Hong, S. G. Kang (2008) Enhancement of the crack growth resistance of a carbon/epoxy composite by adding multi-walled carbon nanotubes at a cryogenic temperature. Composites Part A **39,** 647..
[3] E. T. Thostenson, C. Li, T. W. Chou (2005) Nano composites in context. Compos Sci Technol **65,** 491.
[4] F. Hussain, M. Hojjati, M. Okamoto (2006) Polymer matrix nano composites processing, manufacturing and application- an overview. J Compos Mater **40,** 1511-75.

4 **Flame propagation rate and LOI of the neat and nano–ATH filled glass/epoxy composites**

Sample ID	Flame propagation rate (mm/sec)	LOI
GEC	0.162	28±0.2
0.125ATHGEC	0.153	30±0.2
0.25ATHGEC	0.148	32±0.2
0.5ATHGEC	0.142	33±0.2

5 **Time-to-ignition and UL 94V rating of the neat and nano-ATH filled glass/epoxy composites**

Sample ID	Time of burn after flame (sec)	Rating
GEC	18	NR
0.125ATHGEC	15	NR
0.25ATHGEC	10	V-0
0.5ATHGEC	8	V-0

[5] S. Y. Fu, X. Q. Feng, Lauke B. (2008) Effects of particle size, particle/matrix interface adhesion and particle loading on mechanical properties of particulate-polymer composites. Composites Part B **39,** 933.
[6] C. J. Schwartz, S. Bahadur (2000) Studies on the tribological behaviour and transfer film-counter face bond strength for polyphenylene sulphide filled with nano scale alumina particles. Wear **237**, 261.
[7] L. Chang, Z. Zhang, C. Breidt (2005) Tribological properties of epoxy nano composites- I. Enhancement of the wear resistance by nano-TiO_2 particles. Wear **258,** 141.
[8] B. Wetzel, F. Haupert, K. Friedrich (2002) Impact and wear resistance of polymer nano composites at low filler content. Polym Eng Sci **42,** 1919.
[9] F. Li, K. Hu, J. Li (2002) The friction and wear characteristics of nanometer ZnO filled polytetrafluoroethylene. Wear **249,** 822.
[10] N. Mohamad, A. Muchtar, M. J. Ghazali (2008) The effect of filler on epoxidised natural rubber-alumina nanoparticles composites. Eur J. Sci Res **24,** 538.
[11] Q. L. Ji, M. Q. Zhang, M. Z. Rong (2004) Tribological properties of surface modified nano-alumina/epoxy composites. J. Mater Sic. **39,** 6487.
[12] G. Shi, M. Q. Zhang, M. Z. Ronga (2004) Sliding wear behaviour of epoxy containing nano-Al_2O_3 particles with different pre-treatments. Wear **256,** 1072.
[13] W. Shen, C. Pan, K. Wu. The study on ablation resistance of epoxy resin based composite in vacuum. In: Proceedings of ICSD-10 conference. Potsdam, Germany, July, (2010) 1.
[14] G. Peng, L. Gao, Z. Zhan (2009) Wear behaviour of $Al(OH)_3$-GF/epoxy composites in low velocity. Polym Bull **63,** 911.
[15] B. N. Dudkin, G. G. Zainullin, P. V. Krivoshapkin (2008) Influence of nanoparticles and nano fibres of aluminium oxide on the properties of epoxy composites. Glass Phys Chem **34,** 187.
[16] ASTM International. D792: Standard test methods for density and specific gravity (relative density) of plastics by displacement. (2001) 1.
[17] ASTM International. D638: Standard test method for tensile properties of plastics. (2004) 1.
[18] ASTM International. D790: Standard test methods for flexural properties of unreinforced and reinforced plastics and electrical insulating materials. (2003) 1.
[19] D. F. Adams, E. Q. Lewis (1997) Experimental assessment of four composite materials shear test methods. J Test Eval **25** 174.
[20] ASTM International. G99: Standard test method for wear testing with a pin-on-disk apparatus. (2004) 1.
[21] http://rsb.info.nih.gov/ij/ (accessed on 01 March 2013).
[22] J. J. Friel, J. C. Grande, D. Hetzner (2000) A practical guide to image analysis. ASM international, Materials Park, Ohio, USA.
[23] ASTM International. D2863: Standard test method for measuring the minimum oxygen concentration to support candle-like combustion of plastics. (2000) 1.
[24] R. F. Grossman (2007) Handbook of Vinyl Formulating. Hoboken, John Wiley & Sons, Inc., NJ, USA.
[25] Theophanides T (2012) Infrared spectroscopy - materials science, engineering and technology. InTech, Janeza Trdine 9, Croatia.
[26] B. I. Kharisov, O. V. Kharissova, U. O. Méndez (2013) Radiation Synthesis of Materials and Compounds. CRC Press, Boca Raton, FL.
[27] Y. Choe, W. Kim (2002) Cure reactions of epoxy/anhydride/(polyamide copolymer) blends. Macromol. Res **10,** 259.
[28] J. Rocks, L. Rintoul, F. Vohwinkel, G. George (2004) The kinetics and me chanism of cure of an amino-glycidyl epoxy resin by a co-anhydride as stu died by FT-Raman spectroscopy. Poly mer **45** 6799.
[29] J. Bijwe, S. Awtade, B. K. Satapathy, (2004) Influence of concentration of aramid fabric on abrasive wear performance of polyethersulfone composites. Tribol Lett **17** 187.
[30] N. Mohan, S. Natarajan, S. P. Babu Kumaresh (2010) Investigation on sliding wear behavior and mechanical properties of jatropha oil cake-filled glass-epoxy composites. J. Am Oil Chem Soc **88** 111.
[31] P. Poomalai, Siddaramaiah, B. Suresha, (2008) Mechanical and three-body abrasive wear behaviour of PMMA/TPU blends. Mater Sci Eng, A **492** 486.
[32] B. Shivamurthy, K. U. Bhat, S. Anandhan (2013) Mechanical and sliding wear properties of multi layered laminates from glass fabric/graphite/epoxy composites. Mater Des **44**: 136.
[33] L. N. Chang, M. Jaafar, W. S. Chow (2012) Thermal behavior and flammability of epoxy/glass fiber composites containing clay and decabromodiphenyl oxide. J Therm Anal Calorim doi: **10**.1007/s10973-012-2681-z.
[34] S. V. Levchik, E. D. Weil (2004) Thermal decomposition, combustion and flame-retardance of epoxy resins-a review of the recent literature. Polym Int **12** 1901.
[35] R. Hull, A. Witkowski, L. Hollingbery (2011) Fire retardant action of mineral fillers. Polym Degrad Stab **96** 1462.